Decomposition of 5-Nitro-2,4-dihydro-3*H*-1,2,4-triazol-3-one (NTO): Energetics Associated with Several Proposed Initiation Routes

C. Meredith, T. P. Russell, R. C. Mowrey, and J. R. McDonald*

Naval Research Laboratory, Chemistry Division, Code 6110, Washington, D.C. 20375-5342

Received: August 8, 1997; In Final Form: October 20, 1997[⊗]

Initial steps for several proposed decomposition mechanisms of NTO have been studied theoretically in order to determine the energies of various reaction intermediates. The methods applied were restricted Hartree−Fock self-consistent field (SCF), single- and double-excitation configuration interaction (CISD), CISD corrected for unlinked quadruple excitations (CISD+Q), and coupled cluster including all single and double substitutions (CCSD) with a double-ζ plus polarization (DZP) basis set. Harmonic vibrational frequencies were computed to characterize the species at the stationary points. The previously reported mechanisms examined include decomposition initiated by C−NO_2 homolysis, migration of ring substituents, and ring-opening processes. On the basis of the energetics of the various schemes, our computations suggest that C−NO_2 bond homolysis is the most probable initial step for unimolecular decomposition of NTO.

Introduction

5-Nitro-2,4-dihydro-3*H*-1,2,4-triazol-3-one (NTO) was developed at Los Alamos National Laboratory in 1983 as a potential high-performance insensitive energetic material (ref 1 and references therein). It was found to possess desirable explosive properties such as high energy release on decomposition and high detonation velocity. In addition, NTO exhibits good thermal stability[2] and low chemical sensitivity to radiation damage[3] and is relatively insensitive to impact and shock.[2,4]

NTO contains a triazole ring with a keto carbon, C_3, and a nitro group substituted at carbon C_5 (Figure 1). Whereas some researchers have investigated NTO's structural parameters,[1,5,6] most have focused on the thermal[2,4,6−14] and photochemical[3,8,15] decomposition of the bulk material. Although the decomposition process has been studied extensively, there is no consensus on the overall mechanism or even on the initial step(s). Numerous pathways are feasible, and experimental evidence in support of several possibilities has been presented.[2−4,6−16]

The principal point of contention concerns the nature of the initial decomposition steps. Studies have shown that an increase in thermal energy may initiate any of the following unimolecular processes: rupture of the ring;[11] homolysis of one or more bonds between the ring atoms and their substituents, leaving the ring intact;[7,10] exchange of two adjacent ring substituents followed by breakdown of the ring;[16] or nitro-nitrite rearrangement.[13] (Bimolecular initiation in the condensed phase also has been proposed[8,12−14] but is not considered here.) Although one of these initiation events may predominate under a given set of experimental conditions, competition among these pathways is likely depending upon the physical environment and the excess energy available.

The present study addresses the energetics of early NTO gas-phase thermal decomposition and, to a lesser extent, the structural characteristics of the NTO molecule. The following account summarizes the principal mechanisms proposed by previous researchers. Except for the recently proposed initiation through nitro−nitrite rearrangement,[13] each of the unimolecular processes described below is examined in this paper.

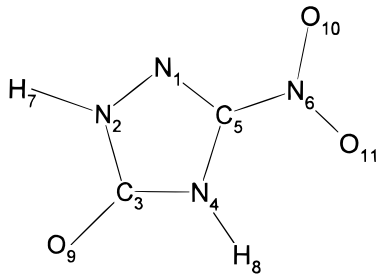

Figure 1. 5-Nitro-2,4-dihydro-3*H*-1,2,4-triazol-3-one (NTO). Theoretical and experimental structural parameters may be found in Table 3.

Proposed Initiation Steps

Homolysis of One or More Bonds to Ring Substituents. Various investigators have asserted that NTO thermal decomposition begins with homolysis of the C−NO_2 bond only, the C−NO_2 and N−H bonds simultaneously (i.e., loss of HONO), or the C−NO_2H linkage following migration of the hydrogen substituent to the vicinal nitro group. Östmark, Bergmann, and Åqvist's GC/MS analysis,[7] for example, shows features consistent with a primary loss of NO_2 and/or HONO and subsequent formation of 2,4-dihydro-3*H*-1,2,4-triazol-3-one (TO) (Figure 2). In addition, the X-ray diffraction (XRD), spectroscopic, and thermal analysis studies of Prabhakaran et al.[6] indicate that the initial changes in thermal decomposition are correlated with loss of the C−NO_2 functionality.

In 1994, Williams, Palopoli, and Brill[9] published results that ostensibly refuted the hypotheses of Östmark et al.[7] and Prabhakaran et al.[6] Using infrared (IR) spectroscopy to examine the initial gaseous products of NTO decomposition under rapid heating (300 °C s^{-1}) as a function of pressure, they found *neither* NO_2 nor HONO initially.

Shortly thereafter, Oxley, Smith, Zhou, and McKenney[10] studied the decomposition of NTO over the temperature range 220−280 °C. Their proposed high-temperature mechanism,

[⊗] Abstract published in *Advance ACS Abstracts,* December 15, 1997.

S1089-5639(97)02602-9
Published on Web 01/08/1998

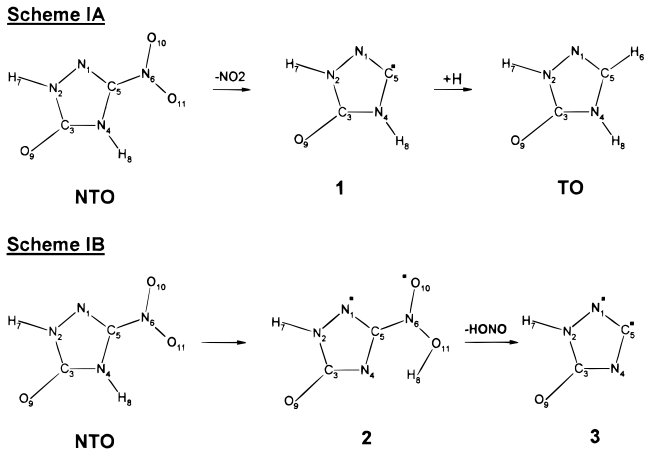

Figure 2. Proposed decomposition pathways for NTO. Scheme I depicts two major pathways initiated by loss of NO_2 (Scheme IA) or HONO (Scheme IB); ref 7, 10.

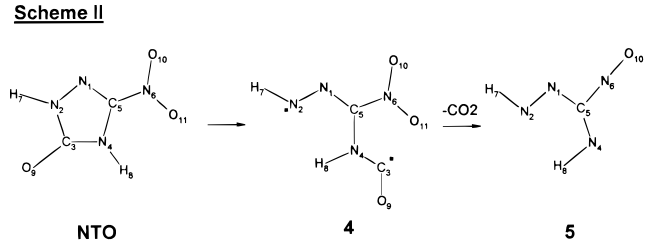

Figure 3. Proposed decomposition pathways for NTO. Scheme II is a ring-opening mechanism; ref 11.

which is initiated by loss of HONO or NO_2, is consistent with the findings of Ostmark et al.[7] However, Oxley and co-workers also documented both primary and secondary deuterium kinetic isotope effects (DKIEs), leading them to conclude that hydrogen transfer is involved as a rate-limiting process at lower temperatures. A subsequent study by Oxley, Smith, Yeager, Rogers, and Dong[16] suggested two distinct mechanisms. One pathway proceeds by means of CO_2 and N_2 evolution, a route that would account for the previously reported DKIE.[8,10] They also speculate, however, that nitro group migration from the ring carbon (C_5) to an adjacent ring nitrogen (N_4) may occur.

Prior to the aforementioned studies, Menapace, Marlin, Bruss, and Dascher,[8] who studied NTO decomposition under both photochemical and thermal stimuli, proposed a bimolecular mechanism consistent with the early loss of HONO. They postulate that the same intermolecular initiation step occurs under either stimulus.

Rupture of the Triazole Ring. Beardall, Botcher, and Wight[11] recently published a study of NTO thermal decomposition using pulsed IR laser pyrolysis of thin films and Fourier-transform IR spectroscopy for product analysis. Unlike previous investigators, they observed appreciable quantities of CO_2, which they surmise were formed by *intramolecular* oxidation by the nitro group at the keto carbon. Moreover, they detected neither NO_2 nor HONO as primary decomposition species. Because no previously proposed mechanism could account for their observations, they suggested a novel ring-opening mechanism (Figure 3) that they have since repudiated.[12]

Exchange of the Nitro Substituent with the Vicinal Hydrogen Substituent. Oxley et al.,[16] in order to reconcile their findings with those of Wight and co-workers,[12] proposed as an initial step the exchange of the nitro group with the vicinal hydrogen substituent, yielding a higher energy intermediate (Figure 4). This exchange presumably is followed by a

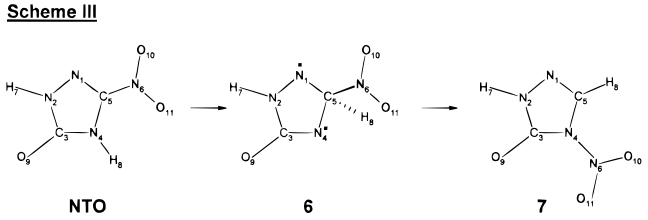

Figure 4. Proposed decomposition pathways for NTO. Scheme III features a nitro migration followed by breakdown of the triazole ring; ref 16.

unimolecular breakdown of the triazole ring, yielding CO_2 and other products.

Nitro−Nitrite Rearrangement. McMillen, Erlich, He, Becker, and Shockey[13] recently completed a laser ionization mass spectrometric analysis of fracture-induced and thermal NTO decomposition. Their results suggest several decomposition pathways, all of which feature a nitro−nitrite rearrangement followed by NO loss. The authors report that, although the initial step may occur either as a single unimolecular reaction or a dissociation−recombination sequence, in either case their data are consistent with the major experimental observations of previous researchers.

Bimolecular Routes: Collisional Interactions. NTO decomposition due to bimolecular interactions also has been proposed. The Wight group[12] recently confirmed their previous identification[11] of CO_2 as the initial gas-phase product. This time, however, their kinetic data indicated an initial bimolecular step. Their revised mechanism, which features oxygenation by the nitro group at the keto carbon of a neighboring molecule, is consistent with their observations of CO_2 as the only gas-phase molecule released at threshold and a quadratic dependence on the NTO concentration. Another bimolecular mechanism was reported in the aforementioned EPR study of Menapace et al.,[8] who found the initial decomposition step to be a hydrogen abstraction from either a neighboring NTO molecule or a solvent molecule, yielding HONO and a cyclic open-shell intermediate.

The most recent experiments suggesting bimolecular initiation are the laser-induced decomposition studies of Garland, Ladouceur, and Nelson.[14] These researchers propose that the nitro−nitrite transformation simultaneously observed by McMillen et al.[13] occurs via an intermolecular process with a net loss of an oxygen atom to yield nitroso-TO (*m*/*z* 114). They also note, however, that both NO_2 loss and nitro−nitrite rearrangement with subsequent loss of NO represent plausible early unimolecular steps.

Previous Theoretical Studies

Although NTO decomposition has been studied experimentally for many years, comparatively few quantum mechanical studies of NTO have been reported. Ritchie[17] used the SCF method in an early study of the structure and energy of NTO. The molecular geometry was optimized using a 3-21G basis set, and single-point energies were evaluated with a 6-31G* basis. Östmark et al.[7] include, in their experimental NTO study, calculations designed to verify the initial decomposition steps and to explain the high stability of NTO. Their method was the semiempirical modified neglect of differential overlap (MNDO) with an unrestricted Hartree−Fock wave function. Their results confirm that "the weak part of the NTO molecule is the C−NO_2 bond," a finding that lends credence to their contention that decomposition begins with C−NO_2 homolysis.

Harris and Lammertsma[18] recently published a thorough study of tautomerism, ionization, and bond dissociations of NTO.

TABLE 1: DZP Energies (in atomic units; 1 hartree = 627.51 kcal mol^{-1}) for NTO and Selected Proposed Decomposition Intermediates and Products[a]

compound(s)	RHF	CISD//RHF	CISD+Q//RHF	CCSD//RHF
NTO	−519.253 369	−520.337 225	−520.552 371	−520.674 516
1	−315.089 189	−315.822 342	−315.940 814	−315.981 662
TO	−315.754 245	−316.508 527	−316.631 593	−316.673 397
2	−519.211 469	−520.271 444	−520.480 220	−520.607 172
3	−314.461 515	−315.176 488	−315.292 296	−315.334 258
4	−519.125 593	−520.191 592	−520.404 374	−520.534 381
5	−331.496 405	−332.264 927	−332.397 084	−332.448 210
6	−519.149 363	−520.204 602	−520.413 420	−520.534 788
7	−519.219 834	−520.303 200	−520.518 384	−520.640 745
NO_2	−204.070 599	−204.525 575	−204.577 776	−204.579 000
HONO	−205.157 426	−205.157 426	−205.211 439	−205.214 124
CO_2	−187.675 722	−188.088 308	−188.130 965	−188.130 989
H	−0.497 637			−0.497 637
1 + NO_2 + H		−520.722 656	−520.933 848	
3 + HONO		−520.212 019	−520.422 062	
5 + CO_2		−520.235 876	−520.449 603	

[a] Zero-point vibrational energies have been omitted.

Their study employed molecular orbital SCF and MP2 theories and the B3LYP hybrid density functional using the 6-31+G* and 6-311+G** basis sets. They examined 15 tautomers, radicals, and anions of NTO and concluded that the planar keto NTO tautomer was the most stable. They also estimated N−H and C−NO_2 bond dissociation energies for the planar keto tautomer as 93 and 70 kcal mol^{-1}, respectively. Although Harris and Lammertsma advise that Botcher et al.'s recent experimental findings[12] conflict with their results, they nevertheless propose that C−NO_2 bond cleavage is the likely initial decomposition step at high temperatures, whereas hydrogen atom transfers may play a key role in the condensed phase. Moreover, because several NTO tautomers are energetically accessible, these may prove to be significant in the condensed phase, where they can be formed by a base-catalyzed mechanism.

Shortly after Harris and Lammertsma's paper appeared, Sorescu, Sutton, Thompson, Beardall, and Wight[19] published additional calculations on NTO. This information was presented as part of a study comparing theoretical and experimental NTO force fields. The theoretical force field for gas-phase NTO was determined at the 6-311G** MP2 level of theory. Vibrational frequencies were obtained for both pure NTO films and NTO molecules isolated in an argon matrix at 21 K. Sorescu et al. constructed their force field for solid-state NTO using frequencies for NTO films and scaled ab initio vibrational frequencies. On the basis of the differences between their solid state and gas-phase results, they concluded that the local molecular environment and the sample preparation procedures exert a marked influence on the spectral characteristics of NTO.

The present ab initio investigation of NTO and its early decomposition products seeks to provide insight into the energetic feasibility of all but one of the proposed unimolecular initiation steps discussed above. (The recently proposed nitro−nitrite rearrangement[13,14] is not considered here.) Our approach is to investigate the unimolecular energetics of the steps presented and to determine whether the pertinent molecular species correspond to stable minima or transition states. In this study, SCF geometry optimizations of all proposed intermediates are performed, and the stationary points obtained are characterized through computation of second derivatives along with their associated harmonic vibrational frequencies. In addition, CISD, CISD+Q, and CCSD single-point energies are evaluated at all SCF stationary points, thus providing more reliable relative energies than those previously obtained from SCF energies alone.

Theoretical Methods

Ab initio quantum mechanical methods have been used in this study. Geometries for all stationary points were computed using restricted Hartree−Fock self-consistent-field (SCF) analytic gradient methods.[20] Analytic second-derivative methods[21] were applied to determine which structures correspond to potential minima. The theoretical harmonic vibrational frequencies for NTO, TO, and **7** are scaled by a factor of 0.91 to account for the effects of anharmonicity and electron correlation.[22] Single-point energies for all species included in Schemes I−III were evaluated using the configuration interaction with single and double excitations (CISD)[23] and the coupled cluster with single and double substitutions (CCSD)[24] methods. In the CISD and CCSD energy calculations, configurations representing excitations from the core orbitals into the highest-lying virtual orbitals were deleted. The effect of unlinked quadruple excitations on the CISD energies was estimated by incorporating the Davidson correction;[25] the corresponding energies are denoted CISD+Q.

The basis set used in this research was the standard double-ζ (DZ) set of Huzinaga[26] and Dunning,[27] which was augmented by adding one set of polarization functions (DZP) to each atom. The polarization function orbital exponents were $\alpha_p = 0.75$ for hydrogen and $\alpha_d = 0.85$ for the second-row atoms. The *d* functions were the five-component spherical harmonics. The DZP CISD wave function (C_s symmetry) for NTO includes 1 585 159 configuration state functions, whereas that of the C_1 symmetry species **2** consists of 3 356 916 configurations. All studies were performed with the PSI system of programs[28] using an IBM RS/6000 or an SGI/IRIX workstation.

Results

NTO, a planar molecule containing a five-membered heterocyclic ring with one nitro substituent (see Figure 1), is an extraordinarily stable high-energy compound. As noted in the Introduction, several thermal decomposition pathways for NTO have been proposed. In this study, the gas-phase energetics of the early steps of Schemes I−III are examined at both the restricted Hartree−Fock SCF and at correlated levels of theory and will be discussed in turn. In addition to NTO, 12 proposed decomposition intermediates and early products have been characterized. The absolute energies for these compounds are listed in Table 1. The energy changes associated with the early decomposition steps of Schemes I−III are presented in Table 2.

TABLE 2: Energetics Associated with the Early Steps of Several Proposed NTO Decomposition Pathways[a]

step or rxn	ΔE_{SCF}	ΔE_{CISD}	ΔE_{CISD+Q}	ΔE_{CCSD}
Scheme IA				
NTO $\rightarrow NO_2 + \mathbf{1}$	+54.4	+66.1	+68.6	+67.1
$\mathbf{1} + H \rightarrow TO$	−97.1	−109.0	−112.2	−113.8
NTO + H → NO_2 + TO	−42.7	−42.9	−43.6	−46.7
Scheme IB				
NTO → **2**	+24.3	+39.3	+43.3	+40.3
2 → **3** + HONO	+33.4	+35.9	+35.1	+34.4
NTO → **3** + HONO	+57.7	+75.2	+78.4	+74.7
Scheme II				
NTO → **4**	+76.5	+87.7	+89.2	+84.2
4 → CO_2 + **5**	−30.5	−29.1	−29.7	−29.4
NTO → CO_2 + **5**	+46.0	+58.6	+59.5	+54.8
Scheme III				
NTO → **6**	+63.9	+81.8	+85.8	+86.3
6 → **7**	−43.1	−60.8	−64.8	−65.4
NTO → **7**	+20.8	+21.0	+21.0	+20.9

[a] The relative energies (in kcal mol^{-1}) for all pathways are determined at the RHF, CISD, CISD+Q, and CCSD levels of theory and include the effects of the zero-point vibrational energies. All CISD, CISD+Q, and CCSD values are based on energies evaluated at the appropriate RHF stationary point(s).

As stated above, the geometries for all species were optimized at the SCF level of theory only. Single-point energies were then evaluated at the SCF geometries using CISD and CCSD wave functions. To test the assumption that the use of single-point energies introduces minimal error into the energy calculations, CISD- and CCSD-optimized geometries for the species TO were obtained, and the resulting energies were compared with the single-point energies evaluated at the SCF geometries. The difference between the CISD single-point energy and that of the fully optimized CISD geometry is 1 kcal mol^{-1}. The corresponding CCSD discrepancy is 3 kcal mol^{-1}. Therefore, it is presumed that the change in ΔE values in Table 2 due to refining the geometries at the correlated levels of theory would be less than ~3 kcal mol^{-1}.

NTO's predicted geometrical parameters are presented and compared with theoretical bond lengths of several key intermediates in Table 3. Scaled DZP SCF harmonic vibrational frequencies, infrared (IR) intensities, and zero-point vibrational energies (ZPVEs) for NTO, TO, and structure **7** are listed in Table 4. Also included in this table are experimental IR vibrational frequencies, obtained from a recent paper by the Wight group.[19]

Discussion

Structural Parameters. *General Considerations.* Crystalline NTO may exist in either of two polymorphs, which are denoted α (triclinic) and β (monoclinic). Whereas most experimental mechanistic studies have been carried out on the α polymorph, the single-crystal X-ray diffraction data of Lee and Gilardi[1] represent structural parameters of the β-form of NTO. In comparing theoretical gas-phase NTO bond lengths with the parameters of β-NTO, some general trends are apparent. First, with one exception, the five bond lengths comprising the heterocyclic ring compare favorably with the experimental data; the average difference between the theoretical and experimental bond lengths comprising the ring structure is 1%. Because SCF theory is well-known to underestimate bond lengths (and therefore overestimate vibrational frequencies), the predicted bond lengths are on the short side; inclusion of electron correlation would improve this estimate, most likely yielding longer bonds that would perhaps exceed the experimental bond lengths. Among the ring bonds, the greatest discrepancy (2.3%) is seen for the only π-bond, $C_5{=}N_1$; the SCF value here is especially unreliable because electron correlation is necessary to provide an adequate description of an electron-rich bond. With the exception of the bonds to the hydrogen atoms, the deviations from the corresponding experimental values are only slightly greater for the remaining bonds. The error in the computed N−H bond lengths cannot be ascertained because of uncertainties in determining the precise location of the hydrogen atoms using X-ray diffraction methods.

TABLE 3: Comparison of Selected DZP SCF Structural Parameters (Bond Lengths in Å) for NTO and the Intermediates 1, 2, TO, 3, and 7[a]

	exptl	theoretical					
parameter	NTO	NTO	**1**	**2**	TO	**3**	**7**
N(1)−N(2)	1.369	1.354	1.384	1.318	1.369	1.323	1.366
N(2)−C(3)	1.367	1.372	1.358	1.402	1.358	1.403	1.357
C(3)−N(4)	1.378	1.382	1.393	1.402	1.380	1.420	1.419
N(4)−C(5)	1.349	1.361	1.359	1.267	1.371	1.250	1.394
N(1)−C(5)	1.290	1.260	1.253	1.402	1.270	1.391	1.261
C(3)−O(9)	1.226	1.192	1.196	1.181	1.200	1.179	1.184
N(2)−H(7)	0.876	0.995	0.994	0.997	0.994	0.997	0.995
N(4)−H(8)	0.915	0.997	0.995		0.995		
C(5)−N(6)	1.447	1.446		1.381			
N(6)−O(10)	1.218	1.186		1.259			1.181
N(6)−O(11)	1.217	1.200		1.353			1.197
O(11)−H(8)				0.950			
C(5)−H(6)					1.072		1.069
N(4)−N(6)							1.369

[a] The experimental parameters represent the single-crystal x-ray structure of the β (monoclinic)-form of NTO (see ref 1). The first five bonds listed comprise the triazole ring.

On the basis of valence bond theory, NTO—a monocyclic system with one π bond and three lone pairs among the ring atoms—is unlikely to benefit energetically from the extra stabilization produced by π-electron delocalization. Moreover, one *would not* expect the entire molecule to be planar. For the purposes of the Hückel $4n + 2$ rule, however, the out-of-plane nitrogen lone pairs may be regarded effectively as π-electrons; hence, there are six π or π-like electrons, thus satisfying the Hückel criterion for aromaticity. Both theory and experiment confirm that NTO is a planar species, thus implying significant delocalization of π-electrons. An analysis based on absolute magnetic shielding[29] confirms that NTO indeed exhibits significant aromatic character. This effect partially accounts for its unusual stability.

As stated previously, NTO's structural parameters have been predicted at the SCF level only (see Table 3). TO's, on the other hand, also were determined at correlated levels of theory. Comparison of the differences between SCF and CCSD geometries for TO allows us to extrapolate to produce estimates of NTO's geometrical parameters at higher levels of theory. Considering only the bond lengths comprising TO's triazole ring, the four single bonds are predicted to be 0.8−1.7% longer (CCSD) and the double bond is predicted to be almost 3% longer than the corresponding SCF bond lengths. In addition, the π-bond is predicted to be 1.305 Å (CCSD), a value that agrees well with NTO's crystalline bond length of 1.290 Å.[1]

Geometries of Key Intermediates. The process NTO → **1** → TO (Scheme IA) is characterized by subtle redistribution of electron density within the triazole ring, resulting in an overall relaxation of the ring. For example, the bond length C_5-N_4

TABLE 4: Scaled Theoretical Frequencies (cm^{-1}) and IR Intensities (km mol^{-1}) for NTO, TO, and 7[a]

NTO				TO		str **7**	
freq	int	assignment	exptl[b]	freq	int	freq	int
3574	(167)	N_2-H		3592	(129)	3578	(166)
3559	(211)	N_4-H	3489	3578	(144)	3177	(18)
1837	(1032)	C═O	1789	3137	(<1)	1872	(1066)
1727	(151)	C═N + NO asym	1768	1813	(980)	1704	(177)
1697	(513)	NO asym + C═N	1563	1669	(67)	1684	(171)
1529	(242)	NO sym + $C-NO_2$	1463	1410	(47)	1435	(529)
1439	(157)	NO sym + C_5N_4	1361	1398	(0)	1413	(24)
1401	(6)	rocking H_7	1338	1338	(28)	1355	(273)
1301	(57)	$C_3-N_4 + C_3-N_2$	1257	1231	(25)	1267	(16)
1212	(3)	rocking H_8	1174	1101	(1)	1212	(46)
1124	(33)	N−N	1085	1051	(49)	1183	(6)
1006	(16)	ring def 2	991	996	(26)	1089	(32)
987	(21)	$C_3-N_4 + C_3-N_2$	971	919	(37)	896	(43)
850	(62)	NO_2 scissors	822	898	(14)	887	(14)
806	(5)	oop C_5	738	777	(26)	860	(106)
769	(29)	oop O_9		736	(10)	805	(34)
749	(32)	ring def 1	730	641	(13)	753	(25)
639	(16)	ring tors (1 + 2)	613	481	(12)	745	(23)
578	(9)	NO_2 rocking	573	474	(270)	624	(44)
491	(261)	oop H_8	512	374	(5)	613	(25)
464	(9)	rocking O_9		190	(29)	478	(2)
416	(2)	oop H_7 + oop H_8				404	(1)
408	(<1)	$C-NO_2$ str				403	(113)
282	(39)	ring tors 2 + oop H_7				231	(3)
203	(6)	rocking N_6				182	(15)
140	(<1)	ring tors 2				116	(<1)
70	(0)	tors z				63	(<1)
ZPVE (kcal mol^{-1})		41.8		39.8		41.5	

[a] Infrared intensities (km mol^{-1}) are in parentheses. Experimental fundamental vibrational frequencies for NTO also are included. [b] NTO/Ar matrix experiment. See ref 19.

changes only slightly in response to the nitro substituent elimination and subsequent addition of a hydrogen atom.

The most significant geometry change during the process NTO → **2** → **3** (Scheme IB) is contraction of the C_5-N_4 bond, with a concomitant lengthening of the adjacent ring bonds C_5-N_1 and C_3-N_4. The C_5-N_6 bond also contracts substantially before rupture and release of HONO. This finding, which at first glance may seem counterintuitive, can be attributed to redistribution of electron density caused by bond formation between the migrating hydrogen atom and oxygen O_{10}. Because of their high electronegativities, the nitro group's oxygen atoms tend to accumulate a partial negative charge by withdrawing electron density from the nitrogen atom. In **2**, for atom O_{11} this is satisfied, in part, by transfer of electron density from H_8. This reduces the amount of electron density transferred from N_6 to O_{11} relative to NTO. This excess electron density results in the formation of a stronger C−N bond and a reduction in the internuclear separation.

To help elucidate the relationship between the proposed intermediate **2** and the putative products, **3** and HONO, the equilibrium geometry of the latter was obtained and then compared with the NO(OH) group of species **2**. Except for the terminal NO bond, which lengthens in response to OH bond formation, the geometry of this group is strikingly similar to that of HONO.

The formation of the intermediate **7** from NTO (Scheme III) also is characterized by a redistribution of ring electron density. The most notable individual features here are the elongations of the bonds C_5-N_4 (from 1.361 to 1.394 Å) and C_3-N_4 (from 1.382 to 1.419 Å).

Vibrational Spectra. Theoretical harmonic vibrational frequencies from SCF second derivatives were determined for NTO, TO, and **7**; these were scaled as described in the Theoretical Methods section. The scaled NTO frequencies compare favorably with the Wight group's recent experimental spectrum[19] (see Table 4). Due to NTO's low symmetry, there is considerable mixing among several vibrational modes, thus complicating assignment of the theoretical frequencies. To our knowledge, experimental IR vibrational spectra for TO and **7** have not been reported.

Consideration of Proposed Mechanisms. *Scheme I*. NTO unimolecular decomposition pathways are initiated by NO_2 or HONO loss (Schemes IA and IB, respectively) through homolysis of the bond connecting the substituent to the triazole ring. In the former case, only the $C-NO_2$ bond breaks, yielding a cyclic doublet intermediate (**1**). This intermediate then accepts a hydrogen atom to yield the stable species TO, leading eventually (in experimental studies) to the formation of a solid organic residue. A competing pathway, not considered explicitly here, is the free radical polymerization of the doublet intermediate to yield $(C_2H_2N_3O)_n$, a species containing heterocyclic rings joined by oxygen ether linkages.

The alternate route 1B involves a formally spin-forbidden internal hydrogen transfer from ring nitrogen N_4 to the adjacent carbon C_5's nitro substituent as the initial step. This results in a cyclic triplet intermediate (**2**) with an $-NO_2H$ group bonded to C_5. The newly formed C_5-NO_2H bond then cleaves homolytically, releasing HONO and leaving behind the cyclic triplet **3**. HONO can then return to oxidize this triplet ring, breaking it down to produce the singlet species N_2, CO_2, and H_2C═N−NO.

Our most reliable level of theory predicts a ΔE of 67 kcal mol^{-1} for dissociation of NTO into NO_2 and **1** (Scheme IA). Subsequent formation of TO from **1** and atomic hydrogen yields 114 kcal mol^{-1} for an overall exothermicity of 47 kcal mol^{-1}. Because the energy changes monotonically along the reaction

path in each of these steps, the predicted ΔE values coincide with the kinetic barriers for the forward and reverse reactions.

Regarding the $C-NO_2$ bond energetics, our predicted ΔE (CCSD) for bond dissociation lies between the experimental values of 62 kcal mol^{-1} for nitroethane[30] and 71 kcal mol^{-1} for nitrobenzene.[31] Harris and Lammertsma's recent theoretical findings[18] also are fairly consistent with ours. On the basis of their nitromethane calculations, they infer that the B3LYP/6-311+G** method underestimates the $C-NO_2$ bond energy by about 9 kcal mol^{-1}. To compensate for this, they add 9 kcal mol^{-1} to their computed value of 61.1 for NTO to yield an estimated bond dissociation energy of 70 kcal mol^{-1}. They further note that this compares favorably with the experimental value of 71.4 kcal mol^{-1} for $C-NO_2$ bond dissociation in nitrobenzene.

The dissociation of NTO to produce HONO and **3** (Scheme IB) is more complex. For instance, the elementary step NTO → **2** features concerted rupture of the N−H bond and formation of an O−H bond. A key factor influencing the energetic favorability of this route is the amount of energy required to transfer the hydrogen from N_4 to O_{11}. As might be expected, both the production and subsequent reaction of the internal hydrogen transfer intermediate (**2**) are endothermic.

Whereas the potential energy curve associated with breaking the $C-NO_2$ bond should increase monotonically, loss of HONO from NTO occurs via a spin-forbidden intramolecular hydrogen shift to produce the minimum-energy intermediate **2**. This rearrangement and the ensuing dissociation proceed by way of transition states that cannot be located easily. The predicted ΔE values thus correspond not to energetic barrier heights but rather *lower* bounds to the reaction barriers. We therefore expect the true barriers to the steps comprising Scheme IB to be higher than our predicted ΔE values. The amount of energy required to form **3** and HONO from NTO will be greater than the overall endothermicity of 75 kcal mol^{-1} for the reaction. Consequently, both relative energetics and spin considerations favor Scheme IA over IB.

Scheme II. This ring-opening scheme, which was proposed and then disclaimed by the Wight group,[11,12] is included here for completeness. Relative to the other reaction pathways, this mechanism shows no energetic advantage; the initial bond rupture to produce the triplet transition state species **4** requires 84 kcal mol^{-1}. Because this ring-opening step is spin-forbidden, for an isolated NTO molecule there is no direct connection between NTO and **4**. The initial steps along the intrinsic reaction pathway indicate that **4** connects to a lower energy triplet ring isomer rather than to NTO. In the condensed phase, however, it is conceivable that the triazole ring could break into an open-chain isomer of NTO such as the diradical **4**.

The second step postulated for Scheme II involves oxygen-atom transfer from the nitro to the carbonyl group with subsequent loss of CO_2. Our predicted C_3-O_{10} internuclear separation is 2.6 Å, which suggests that transfer of an oxygen atom and dissolution of the C_3-N_4 bond to form CO_2 is feasible. In addition, we find the sum of the energies for CO_2 and the singlet molecule **5** to be 29 kcal mol^{-1} lower than the energy of **4**, thus indicating an exothermic process overall. Both steps are spin-forbidden for an isolated molecule, however. In any event, nearly all experimental studies involving product analysis have shown *early* production of CO_2.

Scheme III. This proposed decomposition route features an exchange between nitro and hydrogen substituents on adjacent ring carbon and nitrogen atoms. A possible mechanism for such a rearrangement begins with hydrogen atom transfer from the nitrogen to the carbon ring atom, resulting in a triplet intermediate (**6**). Movement of the nitro group out of the plane of the ring and a reduction of the C_5-N_1 bond order accompany the hydrogen transfer. Because two bonds (N−H σ and C−N π) are broken and only one (C−H σ) is formed, the process is endothermic by 86 kcal mol^{-1}. The second step of the exchange reaction involves nitro group transfer to the ring nitrogen atom, N_4. This migration engenders a redistribution of electron density among the ring atoms, leading to a more stable singlet electronic state (**7**). As would be expected, this process is exothermic, releasing 65 kcal mol^{-1} of energy as **7** is formed. Comparison of the energetics for this mechanism with the others indicates that (if the species **6** is an intermediate as seems reasonable) the energy requirements are comparable to those of Scheme II but greater than those of Schemes IA and IB.

We were unable to find evidence in the literature supporting a carbon-to-nitrogen migration of NO_2 for other systems. However, Janssen, Habraken, and Louw report that the reverse reaction—migration of NO_2 from nitrogen to carbon—occurs for *N*-nitropyrazole in various solvents at moderate temperatures.[32] Their experimental observations are consistent with a two-step mechanism in which nitro group migration to the ring carbon atom is followed by relocation of the hydrogen atom to the ring nitrogen. The overall exothermicity was estimated at 15 ± 5 kcal mol^{-1}, a figure that coincides with our predicted *endo*-thermicity of 21 kcal mol^{-1} for the reverse process. Janssen et al. also note that the driving force for the overall isomerization is the greater stability of a *C*-nitro- as compared to an *N*-nitropyrazole. Moreover, this isomerization appeared to be irreversible under their experimental conditions.

The pathway by which the intermediate **7** decomposes is not addressed directly in this study. However, we note that C_3 and O_{11} are only 2.8 Å apart in **7**, thus suggesting the possibility of oxygen atom transfer from the NO_2 group to the carbonyl leading to formation of CO_2.

Conclusions

As previous researchers have noted, definitive answers to the question of how NTO decomposes remain elusive. The experimental observations are somewhat contradictory, suggesting that the decomposition mechanism depends on the specific experimental configuration. Moreover, most experimental studies attempt to extrapolate measurements made at late times to the early decomposition steps. The primary focus of the present study has been to use ab initio quantum chemical methods to compute the energies of NTO and other molecules that may be formed during in its decomposition. A comparison of the energies of these species provides considerable insight into the feasibility of the proposed unimolecular decomposition mechanisms for NTO. This computational approach complements the experimental work done thus far in that it provides information about the amount of energy needed to effect specific rearrangements in an isolated NTO molecule. The present study neglects the interactions between individual NTO molecules, which can be critical in condensed-phase reactions.

The computational results indicate that the unimolecular decomposition pathway with the lowest initial energy requirements is homolysis of the $C-NO_2$ bond (Scheme IA), a process that requires 67 kcal mol^{-1}. The calculations establish a lower bound of 75 kcal mol^{-1} for the related two-step mechanism (Scheme IB) involving loss of HONO from NTO. The actual barrier height can be determined only by locating the transition-state structure along the reaction pathway, a task that exceeded the available resources. A transition state species (**4**) consistent

with that postulated by Wight and co-workers for the ring-opening scheme (Scheme II) was found to lie 84 kcal mol^{-1} above NTO energetically. A possible intermediate species (**6**) for the pathway involving exchange of the NO_2 group and a hydrogen atom (Scheme III) was found to be 86 kcal mol^{-1} above the energy of NTO. This, combined with steric effects, implies that this pathway is unlikely.

Acknowledgment. The authors acknowledge financial support from the Office of Naval Research and the Naval Research Laboratory Program for the Study of Heterogeneous Decomposition of Energetic Materials. T.P.R. also acknowledges financial support from the Office of Naval Research, Program Officer R. S. Miller. This work was performed while one of the authors, C.M., held a National Research Council−Naval Research Laboratory Associateship. We thank R. D. Gilardi for β-NTO structure information and C. A. Thompson for helpful discussions. C.M. is grateful to P. R. Schreiner (University of Göttingen) for evaluating magnetic aromaticity criteria, Y. Xie (University of Georgia) for invaluable technical assistance, and H. F. Schaefer (University of Georgia) for the use of PSI 2.0.8.

References and Notes

(1) Lee, K.; Gilardi, R. *Mater. Res. Soc. Symp. Proc.* **1993**, *296*, 237.
(2) Rothgery, E. F.; Audette, D. E.; Wedlich, R. C.; Csejka, D. A. *Thermochim. Acta* **1991**, *185*, 235.
(3) Beard, B. C.; Sharma, J. *J. Energ. Mater.* **1993**, *11*, 325.
(4) Xie, Y.; Hu, R.; Wang, X.; Fu, X.; Zhu, C. *Thermochim. Acta* **1991**, *189*, 283.
(5) Ritchie, J.; Lee, K.-Y.; Cromer, D. T.; Kober, E. M.; Lee, D. D. *J. Org. Chem.* **1990**, *55*, 1994.
(6) Prabhakaran, K. V.; Naidu, S. R.; Kurian, E. M. *Thermochim. Acta* **1994**, *241*, 199.
(7) (a) Östmark, H. Thermal Decomposition of NTO. FOA Report D-201782.3; National Defense Research Establishment: Sundbyberg, Sweden, Nov. 1991. (b) Östmark, H.; Bergman, H.; Åqvist, G. *Thermochim. Acta* **1993**, *213*, 165.
(8) Menapace, J. A.; Marlin, J. E.; Bruss, D. R.; Dascher, R. V. *J. Phys. Chem.* **1991**, *95*, 5509.
(9) Williams, G. K.; Palopoli, S. F.; Brill, T. B. *Combust. Flame* **1994**, *98*, 197.
(10) Oxley, J. C.; Smith, J. L.; Zhou, Z.; McKenney, R. L. *J. Phys. Chem.* **1995**, *99*, 10383.
(11) Beardall, D. J.; Botcher, T. R.; Wight, C. A. *Mater. Res. Soc. Symp. Proc.* **1996**, *418*, 379.
(12) Botcher, T. R.; Beardall, D. J.; Wight, C. A.; Fan, L.; Burkey, T. J. *J. Phys. Chem.* **1996**, *100*, 8802.
(13) McMillen, D. F.; Erlich, D. C.; He, C.; Becker, C. H.; Shockey, D. A. *Combust. Flame* **1997**, *111*, 133.
(14) Garland, N. L.; Ladouceur, H. D.; Nelson, H. H. *J. Phys. Chem. A* **1997**, *101*, 8508.
(15) Pace, M. D.; Fan, L.; Burkey, T. J. *Mater. Res. Soc. Symp. Proc.* **1996**, *418*, 127.
(16) Oxley, J. C.; Smith, J. L.; Yeager, K. E.; Rogers, E.; Dong, X. X. *Mater. Res. Soc. Symp. Proc.* **1996**, *418*, 135.
(17) Ritchie, J. P. *J. Org. Chem.* **1989**, *54*, 3553.
(18) Harris, N. J.; Lammertsma, K. *J. Am. Chem. Soc.* **1996**, *118*, 8048.
(19) Sorescu, D. C.; Sutton, T. R. L.; Thompson, D. L.; Beardall, D.; Wight, C. A. *J. Mol. Struct.* **1996**, *384*, 87.
(20) Pulay, P. *Modern Theoretical Chemistry*; Schaefer, H. F., Ed.; Plenum: New York, 1977; pp 153−185.
(21) Pople, J. A.; Krishnan, R.; Schlegel, H. B.; Binkley, J. S. *Int. J. Quantum Chem.* **1975**, *S13*, 225. Saxe, P.; Yamaguchi, Y.; Schaefer, H. F. *J. Chem. Phys.* **1982**, *77*, 5647. Osamura, Y.; Yamaguchi, Y.; Saxe, P.; Vincent, M. A.; Gaw, J. F.; Schaefer, H. F. *Chem. Phys.* **1982**, *72*, 131.
(22) Grev, R. S.; Janssen, C. L.; Schaefer, H. F. *J. Chem. Phys.* **1991**, *95*, 5128.
(23) Brooks, B. R.; Laidig, W. D.; Saxe, P.; Goddard, J. D.; Yamaguchi, Y.; Schaefer, H. F. *J. Chem. Phys.* **1980**, *72*, 4625. Rice, J. E.; Amos, R. D.; Handy, N. C.; Lee, T. J.; Schaefer, H. F. *J. Chem. Phys.* **1986**, *85*, 963.
(24) Scheiner, A. C.; Scuseria, G. E.; Lee, T. J.; Rice, J. E.; Schaefer, H. F. *J. Chem. Phys.* **1987**, *87*, 5361.
(25) Langhoff, S. R.; Davidson, E. R. *Int. J. Quantum Chem.* **1974**, *8*, 61.
(26) Huzinaga, S. *J. Chem. Phys.* **1965**, *42*, 1293.
(27) Dunning, Jr., T. H. *J. Chem. Phys.* **1970**, *53*, 2823.
(28) PSI 2.0.8, C. L. Janssen, E. T. Seidl, G. E. Scuseria, T. P. Hamilton, Y. Yamaguchi, R. B. Remington, Y. Xie, G. Vacek, C. D. Sherrill, T. D. Crawford, J. T. Fermann, W. D. Allen, B. R. Brooks, G. B. Fitzgerald, D. J. Fox, J. F. Gaw, N. C. Handy, W. D. Laidig, T. J. Lee, R. M. Pitzer, J. E. Rice, P. Saxe, A. C. Scheiner, and H. F. Schaefer, PSITECH, Inc., Watkinsville, GA 30677, 1995
(29) P. R. Schreiner, unpublished results.
(30) *CRC Handbook of Chemistry and Physics*; 65th ed.; Weast, R. C., Ed.; CRC Press Inc.: Boca Raton, FL, 1984−1985; p F-184.
(31) Renlund, A. M.; Trott, W. M. *Chem. Phys. Lett.* **1984**, *107*, 555.
(32) Janssen, J. W. A. M.; Habraken, C. L.; Louw, R. *J. Org. Chem.* **1976**, *41*, 1758.